Environment. Technology. Resources. Rezekne, Latvia
Proceedings of the 14th International Scientific and Practical Conference. Volume 3, 139-144

Working Regimes for Friction Stir Processing of Aluminium Alloy A6061

Christo Kondoff
Institute of Metal Science, Equipment, and Technologies with Centre for Hydro- and Aerodynamics, Bulgarian Academy of Sciences
Sofia, Bulgaria
hriko61@gmail.com

Rossen Mikhov
Institute of Information and Communication Technologies, Bulgarian Academy of Sciences
Sofia, Bulgaria

Leoneed Kirilov
Institute of Information and Communication Technologies, Bulgarian Academy of Sciences
Sofia, Bulgaria
l_kirilov_8@abv.bg

Radostina Zaekova
Institute of Metal Science, Equipment, and Technologies with Centre for Hydro- and Aerodynamics, Bulgarian Academy of Sciences
Sofia, Bulgaria

Plamen Tashev
Institute of Metal Science, Equipment, and Technologies with Centre for Hydro- and Aerodynamics, Bulgarian Academy of Sciences
Sofia, Bulgaria

Abstract. **Friction Stir Processing (FSP) is a method for solid-state processing, in which a rotating tool is moved onto the material surface to modify the microstructure and thus obtain improved properties of the material surface. We study the effects of FSP on aluminium alloy A6061-T651 using a tool made at the Institute of Metal Science, Equipment, and Technologies with Centre for Hydro- and Aerodynamics (IMSETCHA) of the Bulgarian Academy of Sciences. The tool has a threaded pin with three flutes and a concave shoulder. Optimal process parameters should always be chosen for the treatment of new materials and when a new instrument is used in order to achieve target properties of processed zone. The appropriate properties, like strength, hardness, corrosion resistance, etc. require process parameters that are correctly configured. The most influential parameters on friction stir processing are direction of rotation of the tool, rotation speed, and traverse speed of the processing. In this paper, we investigate the properties of the processed zone for a total of 16 regimes: 4 rotation speeds (900, 1100, 1300, 1500 rpm) and 4 traverse speeds (15, 30, 45, 60 mm/min) using counterclockwise rotation, comparing the results with a previous study using clockwise rotation. Metallographic inquiry, hardness and tribological tests are used to estimate the stirred zone quality.**

Keywords: aluminium alloys A6061, friction stir processing (FSP), friction stir welding (FSW), modelling.

I. INTRODUCTION

Friction Stir Processing (FSP) is an innovative method for solid-state processing. It originates from the Friction Stir Welding (FSW) method proposed in 1991 by The Welding Institute – TWI (UK) [1]. The main principles of FSW are as follows: a rotating tool with a pin and shoulder is set between elements to be joined. The process begins with rotating of the tool and moving it into the direction of welding. The weld is a result of the mixing of the softened material as a result of the rotation and local heating. This simple and efficient way of welding is extensively studied and applied [2], [3].

Several years later, Mishra et al proposed a new method for material processing based on FSW, namely, Friction Stir Processing (FSP) [4]. The idea is by moving the rotating tool onto the material surface to modify the microstructure and thus obtain improved properties of the material surface. FSP was initially designed for superplastic materials. Throughout the years, FSP is also extensively studied [5].

Print ISSN 1691-5402
Online ISSN 2256-070X
https://doi.org/10.17770/etr2023vol3.7235

In this paper we apply a new tool for FSW and FSP made at the Institute of Metal Science, Equipment, and Technologies with Centre for Hydro- and Aerodynamics (IMSETCHA) of the Bulgarian Academy of Sciences. We study the effects of FSP with this tool on aluminium alloy 6061 because this alloy has excellent strength and corrosion characteristics. The investigated alloy has many applications, such as aerospace products, automobile applications, electrical industry, etc.

The paper is organized further as follows. In the next section we give literature overview. Next, the design of the experiments is described, followed by the results, and finally discussion and conclusions.

II. Related Work

Aluminium alloys of all series are widely involved in FSP. Hardened aluminium allows from 6XXX series are subject to FSW and FSP through different instruments and a variety of treatment parameter values. Aluminium alloy A6061 plays a major role in the aerospace, automotive, shipping and other industries because it has good formability, weldability, machinability, corrosion resistance, and good strength compared to other aluminium alloys. It is often used in certain heavy-duty structural applications, such as truck frames, rail coaches, military and commercial bridges, ship building operations, towers and pylons, helicopter rotor skins and many others [6].

Zhang et al. present 3D modelling of material flow in FSW under different process parameters of A6061-T6 alloy, varying tool rotation speed, welding speed, and axial force [7]. A quasi-linear relation is shown between the change of the axial load on the shoulder and the variation of the equivalent plastic strain. The material flow can be accelerated with the increase of the translational velocity and the angular velocity of the pin.

Nam et al. investigate the role of traveling/transversal speed of FSW on the corrosion properties of A6061 aluminium alloy [8]. Four different traveling speeds are examined: base alloy, 40, 60 and 80 mm/min. The electrochemical tests show that increasing of the speed improves corrosion resistance. Another effect is the decreasing of the grains' size and better homogeneity of the microstructure.

Selvaraj et al. study the mechanism of weld formation during FSW of aluminium alloy [9]. The rolled 6 mm thick plate 6061 is made in the size of 150×75×6 mm. The parameters of the tool are: shoulder radius – 9 mm; pin mean radius – 3 mm; pin length – 5.5 mm; pin taper angle – 10°; normal load – 15.5 kN; rotational speeds – 300-2000 rpm; welding velocities – 300, 600, 900, 1400 and 1800 mm/min. Temperatures at different locations are measured using five K-type thermocouples embedded in the advancing side located at a distance of 4 mm, 7 mm, 10 mm, 15 mm and 25 mm from the centre line of the weld. The process parameters for quality weld are identified. The interface temperature range for defect free weld is 400-525°C.

Leon and Jayakumar investigate mechanical properties of A6061 roll plates joined with FSW [10]. The rotating tool has shoulder diameter 18 mm and pin length 5.5 mm. The probe diameter is 6 mm. Different welds are obtained by varying the rotational speed (720, 910, 1120 and 1400 rpm) and the traverse speeds (16, 20, and 31.5 mm/min). The results show that all the weldments are of high quality. When the rotation speed is more than 1200 rpm, the hardness in the weldment increases. Further, when the traverse speed increases from 16 to 31.5 mm/min, an 80-90% reduction in weldment hardness is observed in comparison to the base metal.

Emamian et al. study the influence of tool pin profile on the friction stir welding of A6061-T6 [11]. Four FSW tools with different pin profiles are made of H13 steel – threaded cylindrical, stepped cylindrical, conical, and square. The experiments are performed with three rotational speeds (800, 1200, 1600 rpm) and three traverse speeds (40, 70, 100 mm/min). The conclusion is that increasing the traverse speed influences the tensile strength. The pin profile has no significant influence on the peak temperature and the threaded shape is more efficient for mechanical properties.

Mugada and Adepu investigate the influence of different polygonal tool pin profiles combined with knurling shoulder for Al-Mg-Si alloy [12]. Several cases are considered: hexagonal, pentagonal, square, triangular and taper cylindrical pins. The square and hexagonal pins provide constant stability force in regard to the weld length/time; the square pin produces welds with better mechanical properties. Uniform mixing and distribution of plasticized material is obtained for the knurling shoulder with square tool pin.

Gadakh and Kumar determine the optimal parameter values for FSW of A6061-T6 aluminium alloy [13]. They experiment with: rotational speed, weld speed, the ratio of shoulder to pin diameter and pin geometry. It is found that the rotational speeds within [710, 1400] rpm with weld speed of 40 mm/min produce defect-free weldments; the taper cylindrical (TC) pin produces better fine-grain structure than straight cylindrical (SC) pin; the ratio $D_{shoulder}/D_{pin} = 3$ produces better mechanical properties and fine-grain structure; and the shoulder diameter 24 mm produces better mechanical properties.

Arora et al. propose a criterion for the design of a tool shoulder diameter [14]. They use a 3D heat transfer and visco-plastic flow model developed earlier [15], [16]. The experiments are performed on A6061 with tool rotational speeds 900, 1200 and 1500 rpm; cylindrical profile with no thread and different shoulder diameters 12 to 27 mm. The formulated criterion is a function of both sticking torque and sliding torque with equal partitioning. The optimum shoulder diameter is defined depending on the maximum value of the criterion.

Takhakh and Abdulla [17] apply FSP to improve the mechanical properties of welded joint of A7075-T651 by adding SiC (silicon carbide) on the compound surface. They use a new type of tool (a hollow tool) where the SiC particles are stored, and try different values of the processing parameters.

Patil et al. [18] propose a hybrid reinforcement approach using FSP. They mix silicon carbide and fly ash particles in order to minimize wear rate and maximize microhardness.

Sharma et al. [19] optimize FSP parameters in order to have defect-free surface composites with uniform particle distribution. The experiments are done by adding silicon carbide particles into the A5083 alloy surface. The authors also experiment with dual-tool processing and tool offset overlapping.

III. Design of the Experiments

In this paper, we investigate a tool, made at IMSETCHA, which has the following geometry (see Fig. 1): it has a threaded pin with three flutes and a concave shoulder. The dimensions are: tapered pin – diameter at the base 5.5 mm; pin length – 4 mm, shoulder diameter – 13 mm.

FSP was applied on a rectangular detail of A6061-T651 aluminium alloy, part of sheet metal with thickness 12 mm and dimensions 100×200 mm. The processing was performed on a machining centre HURCO VMX30 (Fig. 2). The angle between the tool and detail was a constant right angle (90°).

Fig. 1. Friction Stir Processing tool.

Fig. 2. Friction Stir Processing equipment.

For the present experiment, the direction of rotation of the tool was counterclockwise (CCW). The results are compared against prior work of Kondoff et al. [20], where rotation direction had been clockwise (CW).

The most influential parameters on friction stir processing are rotation speed of the tool and traverse speed of the processing. We investigated the properties of the processed zone with 4 rotation speeds and 4 traverse speeds, for a total of 16 regimes:

- rotational speeds: 900, 1100, 1300, 1500 rpm;
- traverse speeds: 15, 30, 45, 60 mm/min.

IV. Results and Discussion

In all speed regimes, all of the investigated properties of the processed zone were considerably better in the experiments with counterclockwise rotation of the tool, as opposed to clockwise rotation.

This improvement is due to fact that the tool is right-hand threaded. Better compaction of the material results from the pressing action of the pin against the inner area of the mixing zone.

A. Metallographic Inquiry

To prepare the detail for analysing, it was cut into strips. The strips were marked, ground, polished and etched for metallographic analysis. To assess the imperfections, which in this case are metal deficiency zones (MDZ), a section was considered for each processing regime.

No MDZ imperfections could be observed with CCW rotation, which is in sharp contrast to the CW results of [20].

From the macrostructural analysis (Fig. 3), it can be seen that the size of the cross section of the stirred zone does not depend on the rotation speed and the processing speed. Regardless of the fact that the processing in the different regimes was carried out sequentially, no increase in the cross section of the stirred zone was observed at subsequently processed locations due to an increase in the temperature of the detail. This is likely due to the high thermal conductivity of the used alloy.

Fig. 4 shows the microstructure of the boundary of the processed zone. The grains of the base metal and the significantly finer grains of the stirred zone are clearly visible. The progressive and rotary movement of the tool leads to the formation of layers, known under the name of “onion rings”. They are clearly distinguishable in Fig. 5. With counterclockwise rotation of the tool, there is a tendency for the boundary between the stirred zone and the base material on the advancing side of the tool to be sharper (Fig. 6), and on the retreating side of the tool to be smoother (Fig. 7).

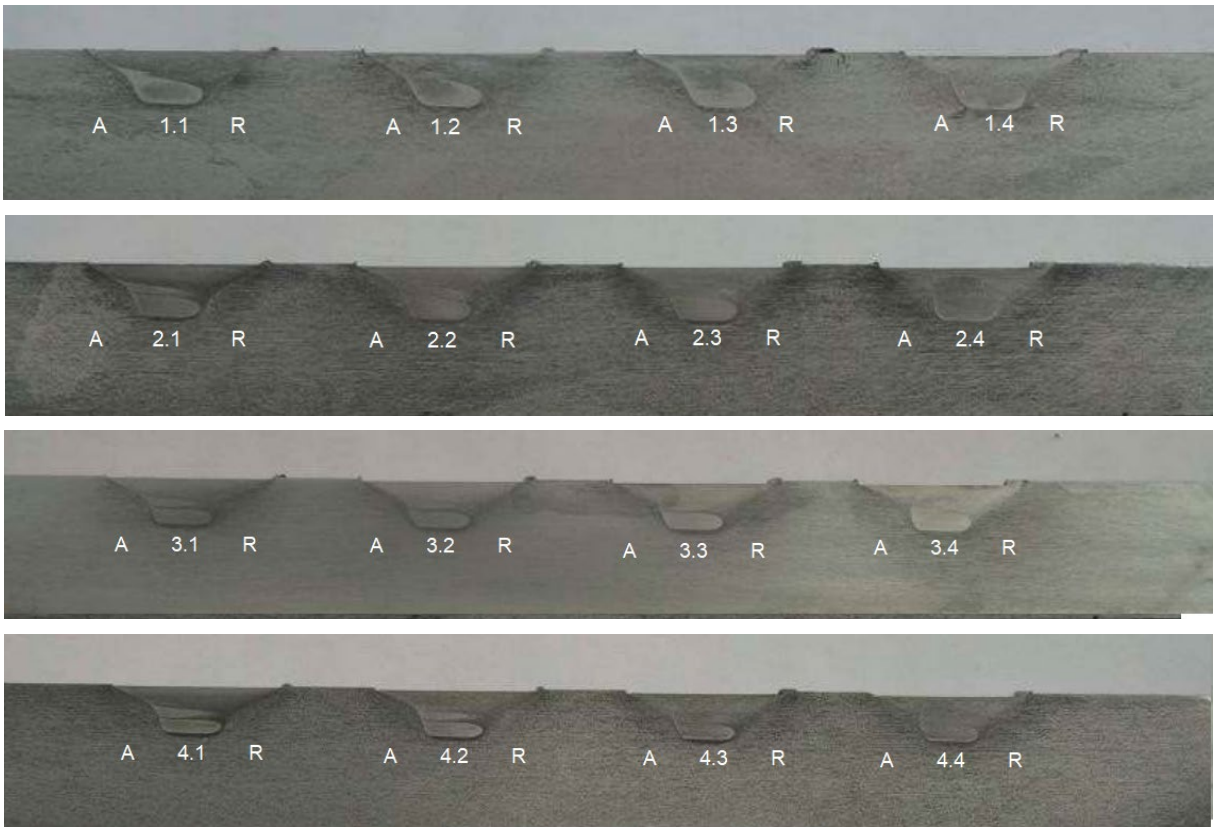

Fig. 3. Macroscopic view of cross sections of the FSP zones at different traverse speeds and rotational speeds, as follows: 1.1 – 15 mm/min, 900 rpm; 1.2 – 15 mm/min, 1100 rpm; 1.3 – 15 mm/min, 1300 rpm; 1.4 – 15 mm/min, 1500 rpm; 2.1 – 30 mm/min, 900 rpm; 2.2 – 30 mm/min, 1100 rpm; 2.3 – 30 mm/min, 1300 rpm; 2.4 – 30 mm/min, 1500 rpm; 3.1 – 45 mm/min, 900 rpm; 3.2 – 45 mm/min, 1100 rpm; 3.3 – 45 mm/min, 1300 rpm; 3.4 – 45 mm/min, 1500 rpm; 4.1 – 60 mm/min, 900 rpm; 4.2 – 60 mm/min, 1100 rpm; 4.3 – 60 mm/min, 1300 rpm; 4.4 – 60 mm/min, 1500 rpm. A – advancing side; R – retreating side.

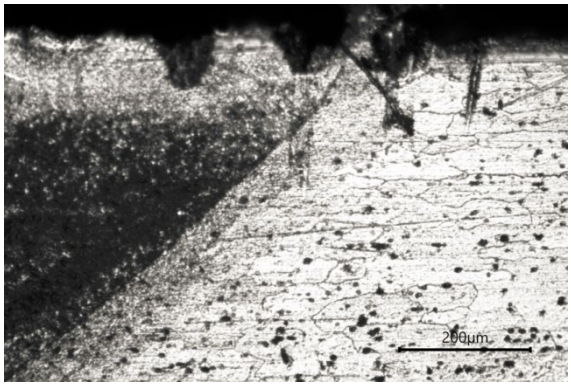

Fig. 4. Grain size of the base and stirred metal (regime 1.1).

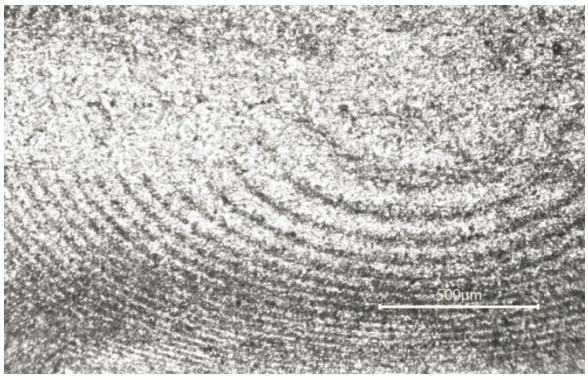

Fig. 5. Onion rings (regime 1.1).

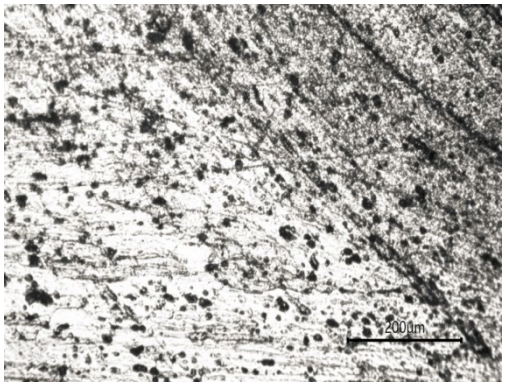

Fig. 6. Smooth border (regime 4.4).

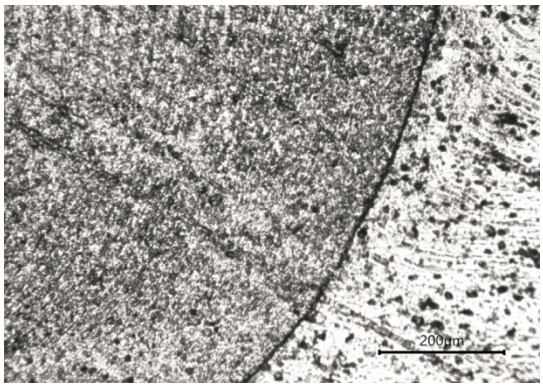

Fig. 7. Sharp border (regime 4.4).

B. Hardness Test

Microhardness (HV) measurements were performed with a Micro-Duromat 4000 (Reichert-Jung), with the following parameters: load – 20 gf; time for reaching the load – 10 s; hold time – 10 s; Vickers indenter. Fig. 8 is an illustration of such a measurement.

The results are listed in Table I. The measurements were performed in three different positions: under the surface, in the middle and at the base. The exact positions are illustrated on Fig. 9.

The highest average hardness is observed at regime 60/900 with a value of 75.8 kgf/mm^2, which is comparable to the hardness of the base material A6061-T651 with an average hardness of 73 kgf/mm^2. In FSP, thermal effect occurs in the stirred zone and the thermally affected zone shows a decrease in hardness, which is due to the partial dissolution of the precipitates from the hard Mg_2Si phase.

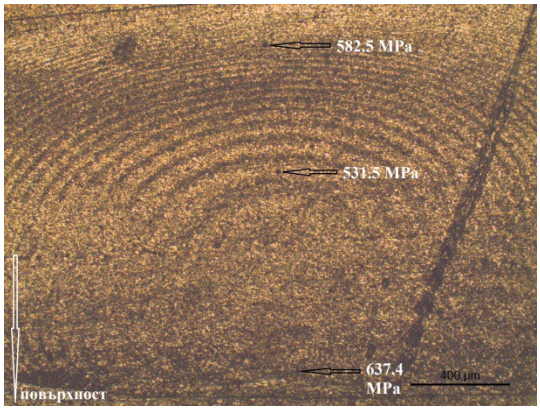

Fig. 8. Image from the microhardness measurement.

C. Tribological Test

Mass wear measurements were performed on a tribological installation with Ducom Pin/Ball disk tester TR-20. The counter body was a disk of special steel EN 31 with hardness 60 HRc. The other parameters were as follows: load – 20 N; speed of the counter body – 80 rpm (1 m/s); trial duration – 10 min; total distance – 600 m.

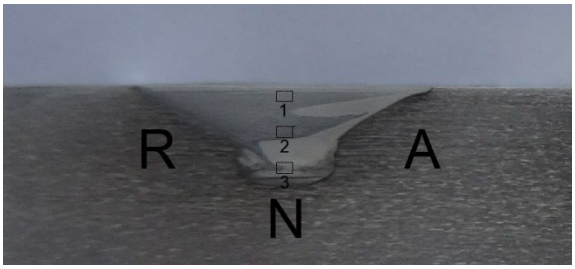

Fig. 9. Positions of the microhardness measurement. A – advancing side; R – retreating side; N – nugget; □1, □2, □3 – measurement positions "below the surface", "in the middle" and "at the base", respectively.

TABLE I MICROHARDNESS HV0.02/10/10

		counterclockwise (CCW) rotation				clockwise (CW) rotation			
		rotation speed, rpm				*rotation speed, rpm*			
		900	1100	1300	1500	900	1100	1300	1500
traverse speed, mm/min		*HV below the surface, kgf/mm²*				*HV below the surface, kgf/mm²*			
	15	62.1	73.6	74.0	71.5	54.6	53.1	49.3	53.8
	30	74.6	65.0	73.7	63.4	37.7	48.3	54.6	48.3
	45	67.6	59.6	63.9	63.7	33.4	48.2	41.1	62.5
	60	73.6	59.1	65.1	53.1	33.0	51.8	54.6	48.1
traverse speed, mm/min		*HV in the middle, kgf/mm²*				*HV in the middle, kgf/mm²*			
	15	65.3	68.4	68.9	70.8	46.0	48.9	49.4	49.8
	30	59.6	54.2	66.8	62.8	46.2	48.9	53.1	49.8
	45	67.6	58.3	64.8	70.9	45.5	45.9	46.5	44.8
	60	81.3	64.4	65.1	59.3	47.9	46.4	50.1	55.5
traverse speed, mm/min		*HV at the base, kgf/mm²*				*HV at the base, kgf/mm²*			
	15	51.4	66.7	68.9	72.4	53.4	51.8	51.4	52.8
	30	61.5	59.4	63.1	73.6	53.8	54.7	52.0	48.1
	45	67.6	59.6	59.6	72.8	53.6	56.9	54.0	55.3
	60	72.5	73.5	67.9	66.6	57.2	55.0	56.5	53.4
traverse speed, mm/min		*HV, average of the 3 positions, kgf/mm²*				*HV, average of the 3 positions, kgf/mm²*			
	15	59.6	69.6	70.6	71.6	51.3	51.3	50.0	52.1
	30	65.2	59.5	67.9	66.6	45.9	50.6	53.2	48.7
	45	67.6	59.2	62.8	69.1	44.2	50.3	47.2	54.2
	60	75.8	65.7	66.0	59.7	46.0	51.1	53.7	52.3

unprocessed material
73.0 kgf/mm^2 (an average of 5 measurements)

Three regimes were selected, and three samples where measured for each regime, from which a mean value was calculated (with the exception of the 15/1500 regime, for which only one sample could be measured). The results are as follows: 15/1500: 1.2 mg; 30/1100: 0.9 mg; 45/1100: 1.27 mg. For comparison, the unprocessed material had a mean mass wear of 1.13 mg (again, an average of 3 measurements).

Due to the large dispersion of the individual results, the tribological analysis establishes that there is no definite pattern regarding mass wear in the investigated regimes.

V. Conclusion

The operating regimes of a tool for friction stir processing on the A6061-T651 aluminium alloy are investigated and analysed. Experiments with four levels of traverse speed and four levels of rotational speed were performed. The main results are as follows:

- The investigated tool in the aforementioned regimes with CCW rotation provides for a defect-free structure of the processed zone.
- In all speed regimes, CCW rotation of the tool is considerably superior to CW rotation, and this was observed with all of the investigated properties of the processed zone.
- The size of the cross section of the stirred zone does not depend significantly on the traverse speed and the rotation speed.
- The regime with highest average hardness of the stirred zone is 60 mm/min / 900rpm, and its hardness is comparable to that of the base material.
- No definite regularity regarding mass wear could be observed.

On the grounds of this experiment, we choose the CCW 60/900 regime as adequate for future applications. In a follow-up work, we plan to investigate the influence of adding Zn and Ti nanopowder to the FSP process under this regime.

VI. Acknowledgement

Christo Kondoff and Plamen Tashev are supported by the Bulgarian NSF under grant KP-06-India-10/02.09.2019 and by the European Regional Development Fund, Operational Programme "Science and Education for Smart Growth 2014-2020", Project CoE "National center of mechatronics and clean technologies" BG05M2OP001-1.001-0008. Leoneed Kirilov is supported by the Bulgarian NSF under grants KP-06-N52/5 and KP-06-N52/7. Rossen Mikhov is supported by the Bulgarian NSF under grant KP-06-N52/7.

References

[1] Z. Ma, "Friction Stir Processing Technology: A Review," Metall. Mater. Trans. A, vol. 39, pp. 642-658, 2008.

[2] H. Luo, T. Wu, P. Wang, F. Zhao, H. Wang, et al., "Numerical Simulation of Material Flow and Analysis of Welding Characteristics in Friction Stir Welding Process," Metals., vol. 9, no. 6, p. 621, 2019.

[3] M. S. S. El-Deeb, L. A. Khorshed, S. A. Abdallah, A. M. Gaafer, and T. S. Mahmoud, "Effect of Friction Stir Welding Process Parameters and Post-Weld Heat Treatment on the Corrosion Behaviour of AA6061-O Aluminum Alloys," Egypt. J. Chem., vol. 62, no. 8, pp. 1367-1375, 2019.

[4] R. S. Mishra, M. W. Mahoney, S. X. McFadden, N. A. Mara, and A. K. Mukherjee, "High strain rate superplasticity in a friction stir processed 7075 Al alloy," Scr. Mater., vol. 42, no. 2, pp. 163-168, 1999.

[5] K. Li, X. Liu, and Y. Zhao, "Research Status and Prospect of Friction Stir Processing Technology," Coatings, vol. 9, no. 2, p. 129, 2019.

[6] Howard Precision Metals Inc., "Applications of 6061 Aluminum Alloy." [Online]. Available: https://www.howardprecision.com/applications-of-6061-aluminum-alloy/ [Accessed: Apr. 27, 2022].

[7] H. W. Zhang, Z. Zhang, and J. T. Chen, "3D modeling of material flow in friction stir welding under different process parameters," J. Mater. Process. Technol., vol. 183, no. 1, pp. 62-70, 2007.

[8] N. D. Nam, L. T. Dai, M. Mathesh, M. Z. Bian, and V. T. H. Thu, "Role of friction stir welding – Traveling speed in enhancing the corrosion resistance of aluminium alloy," Mater. Chem. Phys., vol. 173, pp. 7-11, 2016.

[9] M. Selvaraj, V. Murali, and S. R. K. Rao, "Mechanism of Weld Formation during Friction Stir Welding of Aluminium Alloy," Mater. Manuf. Process., vol. 28, no. 5, pp. 595-600, 2013.

[10] J. S. Leon and V. Jayakumar, "Investigation of mechanical properties of aluminium 6061 alloy friction stir welding," Am. J. Mech. Eng. Autom., vol. 1, no. 1, pp. 6-9, 2014.

[11] S. Emamian, M. Awang, P. Hussai, B. Meyghani, and A. Zafar, "Influences of tool pin profile on the friction stir welding of AA6061," ARPN J. Eng. Appl. Sci., vol. 11, no. 20, pp. 12258-12261, 2016.

[12] K. K. Mugada and K. Adepu, "Effect of knurling shoulder design with polygonal pins on material flow and mechanical properties during friction stir welding of Al−Mg−Si alloy," Trans. Nonferrous Met. Soc. China, vol. 29, no. 11, pp. 2281-2289, 2019.

[13] V. S. Gadakh and A. Kumar, "Friction stir welding window for AA6061-T6 aluminium alloy," Proc. Inst. Mech. Eng. Part B, vol. 228, no. 9, pp. 1172-1181, 2014.

[14] A. Arora, A. De, and T. DebRoy, "Toward optimum friction stir welding tool shoulder diameter," Scr. Mater., vol. 64, no. 1, pp. 9-12, 2011.

[15] R. Nandan, G. G. Roy, T. J. Lienert, and T. Debroy, "Three-dimensional heat and material flow during friction stir welding of mild steel," Acta Mater., vol. 55, no. 3, pp. 883-895, 2007.

[16] R. Nandan, T. J. Lienert, and T. Debroy, "Toward reliable calculations of heat and plastic flow during friction stir welding of Ti-6Al-4V alloy," Int. J. Mater. Res., vol. 99, no. 4, pp. 434-444, 2008.

[17] A. M. Takhakh and H. H. Abdulla, "Improving the Mechanical Properties of Al7075-T651 Welded Joint Using Direct Friction Stir Processing," in Proceedings of the The Second Conference of Post Graduate Researches (CPGR'2017), College of Engineering, Al-Nahrain Univ., Baghdad, Iraq, 2017, pp.6-10.

[18] N. A. Patil, S. R. Pedapati, O. B. Mamat, and A. M. Hidayat Syah Lubis, "Effect of SiC/Fly Ash Reinforcement on Surface Properties of Aluminum 7075 Hybrid Composites," Coatings, vol. 10, no. 6, p.541, 2020.

[19] V. Sharma, Y. Gupta, B. V. M. Kumar, and U. Prakash, "Friction Stir Processing Strategies for Uniform Distribution of Reinforcement in a Surface Composite," Mater. Manuf. Process., vol. 31, no. 10, pp. 1384-1392, 2016.

[20] Ch. Kondoff, V. Dykova, R. Dimitrova, Y. Hadjitodorov, and R. Zaekova, "A Layer Formation on 6061 Aluminum Alloy after FSP," Int. J. NDT Days, vol. 4, pp. 2603-4018, 2021.